AGU PUBLICATIONS

JGR

Journal of Geophysical Research: Space Physics

RESEARCH ARTICLE

10.1002/2016JA023853

Key Points:
- Coincidence of high CME front (or shock) velocity (ΔV) and sufficiently large $-B_z$ corresponds to severe space weather (SvSW)
- Product ($\Delta V \times B_z$) exhibiting a sharp negative spike exceeding a threshold can be used for forecasting SvSW that can cause power outage
- Coincidence of high V (not containing ΔV) and $-B_z$ does not correspond to SvSW; importance of the coincidence is verified using CRCM

Correspondence to:
N. Balan,
balannanan@gmail.com

Citation:
Balan, N., Y. Ebihara, R. Skoug, K. Shiokawa, I. S. Batista, S. Tulasi Ram, Y. Omura, T. Nakamura, and M.-C. Fok (2017), A scheme for forecasting severe space weather, *J. Geophys. Res. Space Physics*, *122*, 2824–2835, doi:10.1002/2016JA023853.

Received 31 DEC 2016
Accepted 11 MAR 2017
Accepted article online 14 MAR 2017
Published online 30 MAR 2017

A scheme for forecasting severe space weather

N. Balan[1,2,3], Y. Ebihara[1], R. Skoug[4], K. Shiokawa[2], I. S. Batista[3], S. Tulasi Ram[5], Y. Omura[1], T. Nakamura[6], and M.-C. Fok[7]

[1]Research Institute for Sustainable Humanosphere, Kyoto University, Kyoto, Japan, [2]Institute for Space-Earth Environment, Nagoya University, Nagoya, Japan, [3]DAE, INPE, São Jose dos Campos, Brazil, [4]Los Alamos National Laboratory, Los Alamos, New Mexico, USA, [5]Indian Institute of Geomagnetism, New Bombay, India, [6]National Institute of Polar Research, Tokyo, Japan, [7]NASA Goddard Space Flight Center, Greenbelt, Maryland, USA

Abstract A scheme is suggested and tested for forecasting severe space weather (SvSW) using solar wind velocity (V) and the north-south component (B_z) of the interplanetary magnetic field (IMF) measured using the ACE (Advanced Composition Explorer) satellite from 1998 to 2016. SvSW has caused all known electric power outages and telegraph system failures. Earlier SvSW events such as the Carrington event of 1859, Quebec event of 1989 and an event in 1958 are included with information from the literature. *Dst* storms are used as references to identify 89 major space weather events ($Dst\text{Min} \leq -100$ nT) in 1998–2016. The coincidence of high coronal mass ejection (CME) front (or CME shock) velocity ΔV (sudden increase in V over the background by over 275 km/s) and sufficiently large B_z southward at the time of the ΔV increase is associated with SvSW; and their product ($\Delta V \times B_z$) is found to exhibit a large negative spike at the speed increase. Such a product ($\Delta V \times B_z$) exceeding a threshold seems suitable for forecasting SvSW. However, the coincidence of high V (not containing ΔV) and large B_z southward does not correspond to SvSW, indicating the importance of the impulsive action of large B_z southward and high ΔV coming through when they coincide. The need for the coincidence is verified using the CRCM (Comprehensive Ring Current Model), which produces extreme *Dst* storms ($<Dst_{MP}> < -250$ nT) characterizing SvSW when there is coincidence.

Plain Language Summary Severe space weather has been known to affect the society by damaging satellite systems and electric power grids. For example, a space weather of the type that occurred in September 1859, if occurs at present times, can cause very serious damages costing up to 1 to 2 trillion U.S. dollars. It is therefore important to study space weather and understand what determines the severity of space weather and whether it can be forecasted and predicted. In this paper we show that the coincidence of the speed of solar storms and southward orientation of the north-south component of the interplanetary magnetic field is responsible for severe space weather at the Earth, and it can be forecasted by 35 min using the data from a satellite that stays at 220 × radius of Earth away from the Earth.

1. Introduction

Space weather of importance here begins with an eruption in the Sun, which leads to a coronal mass ejection (CME) [*MacQueen et al.*, 1974]. CMEs flow out with speed up to thousands of km s^{-1}, density up to 100 cm^{-3}, and IMF (interplanetary magnetic field) up to 100 nT [e.g., *Skoug et al.*, 2004; *Gopalswamy et al.*, 2005]. CMEs while flowing out through the background solar wind of speed ~400 km s^{-1}, density < 5 cm^{-3}, and IMF < 5 nT cause rapid and sometimes severe changes in interplanetary space and in the environment of the planets that encounter the CMEs. The changes in general are known as space weather which also includes the effects of high-speed streams and corotating interaction regions.

Space weather in interplanetary space includes shock waves ahead of high-speed CMEs. Shock waves accelerate background charged particles to high energies over 100 MeV known as solar energetic particles [e.g., *Singh et al.*, 2010]. The highest-energy charged particles can penetrate the skin of space probes and damage spacecraft subsystems and payload instrumentation [e.g., *McKenna-Lawlor*, 2008], even more easily when the charged particles are suddenly accelerated further by a high-speed CME front [e.g., *Balan et al.*, 2014]. Space weather in Earth's environment includes sudden changes in the magnetosphere, ring current, radiation belts, geomagnetic field, and ionosphere and thermosphere [e.g., *Kamide et al.*, 1998; *Wu and Lepping*, 2002; *Ebihara et al.*, 2005; *Liemohn et al.*, 2010; *Balan et al.*, 2010, 2011].

Like Earth's weather, space weather sometimes becomes severe [e.g., *Carrington*, 1859] and causes extensive social and economic disturbances in the current high-tech society [e.g., *Baker*, 2002; *Pulkkinen*, 2007; *Hapgood*, 2011]. It can damage satellite systems [e.g., *Barbieri and Mahmot*, 2004], electric power grids [*Kappenman*, 1996], oil and gas metal pipe lines [*Viljanen et al*., 2006], long-distance communication cables [*Medford et al*., 1989], satellite communication and navigation [*Lanzerotti*, 2001], etc. Studies based on solar flare intensity [e.g., *Shibata and Magara*, 2011], geomagnetic storms [e.g., *Cliver and Svalgaard*, 2004; *Tsubouchi and Omura*, 2007; *Love et al*., 2015], and nitrate content in ice core samples [*Barnard et al*., 2011] suggest that events as severe as or more severe than the famous Carrington event of 1859 [*Carrington*, 1859] can occur again, which would likely cause very serious damage. Indeed, a similar event occurred in July 2012 though was not Earth directed [e.g., *Baker et al*., 2013; *Russell et al*., 2013]. It is therefore important to study space weather, understand what determines the severity of space weather, and forecast (early warning after solar eruption) and predict (long-term warning before solar eruption) severe space weather.

Solar wind and IMF parameters were used earlier for studying solar wind-magnetosphere coupling and *Dst* storm forecasting [e.g., *Burton et al*., 1975; *Scurry and Russell*, 1991; *Klimas et al*., 1997; *Newell et al*., 2007; *Zhu et al*., 2007]. From a knowledge of solar wind velocity (V) and density (N) and IMF B_z, *Burton et al*. [1975] presented an algorithm for forecasting the *Dst* index under quiet and disturbed conditions. *Klimas et al.* [1997] reported a data-driven method for transforming the local-linear forecast model [*Burton et al*., 1975] into both local-linear and nonlinear dynamical analogues of the coupling between the input and output data that enters and forms the forecast model. *Zhu et al*. [2007] presented a multi-input (VB_z and dynamic pressure P) and single-output (*Dst*) discrete time model for *Dst*. Using V, P, IMF intensity, and clock angle (angle between the B_y and B_z components of the IMF), *Newell et al*. [2007] developed empirical functions for the dayside magnetopause magnetic flux merging rate and the efficiency of CME-magnetosphere coupling. However, to our knowledge, the data and their combinations have not yet been used for forecasting severe space weather (SvSW).

Recently, we studied what determines the severity of space weather as experienced by satellite systems and ground systems and reported [*Balan et al*., 2014] that it is the impulsive energy at the CME front (or CME shock) and orientation of IMF B_z at the CME front that determines the severity of space weather. CMEs having a high front (or shock) velocity and sufficiently large IMF B_z southward at the CME front can lead to severe space weather (SvSW). We also introduced a new parameter of *Dst* storms called *mean Dst* during main phase ($<Dst_{MP}> = (-1/T_{MP})\int_{TMP}|Dst|dt$), where $\int_{TMP}|Dst|dt$ is the integral (or sum) of the modulus of *Dst* from main phase onset (MPO) when *Dst* starts decreasing until *Dst*Min. T_{MP} is the main phase duration from MPO to *Dst*Min. $<Dst_{MP}>$ is found to be a unique parameter that can indicate the severity of space weather while other parameters such as *Dst*Min, T_{MP}, and $(dDst/dt)_{MPmax}$ (maximum rate of change of *Dst* during MP) are insufficient [*Balan et al*., 2016]. As defined, a combination of large $\int_{TMP}|Dst|dt$ and short T_{MP} can give high $<Dst_{MP}>$. For example, a super storm (*Dst*Min = −292 nT in Kyoto *Dst*) on 6 November 2001 with a short T_{MP} of 5 h (02–07 UT) gives high $<Dst_{MP}>$ (−259 nT) while the most intense superstorm (*Dst*Min = −422 nT) in the last two solar cycles (20 November 2003) with a long T_{MP} of 12 h (09–21 UT) gives comparatively smaller $<Dst_{MP}>$ (−204 nT). Extreme *Dst* storms having high $<Dst_{MP}>$ (<-250 nT) correspond to B_z southward at the CME front (or CME shock), and storms having smaller $<Dst_{MP}>$ correspond to B_z northward or fluctuating at CME front. All known SvSW events are found to have $<Dst_{MP}>$ <-250 nT. However, $<Dst_{MP}>$ cannot be used for forecasting SvSW events. It will be used here as a reference.

In the present paper we suggest a scheme for forecasting severe space weather (SvSW) by studying all major space weather events in 1998–2016 that produced 89 intense *Dst* storms (*Dst*Min ≤ −100 nT). The Carrington event, the Quebec event, and an event in February 1958 are included. Solar wind and IMF parameters from the ACE (Advanced Composition Explorer) satellite [*McComas et al*., 1998; *Skoug et al*., 2004] are used for developing the forecast scheme. The scheme is then tested. Severe space weather (SvSW) and CME front (or CME shock) velocity (ΔV) are defined in section 2 which includes brief descriptions of all known SvSW events. Data and analysis are described in section 3. The forecast scheme is presented and tested in section 4 and discussed in section 5 which includes model calculations of *Dst* storms using the CRCM (Comprehensive Ring Current Model) [*Fok et al*., 2001].

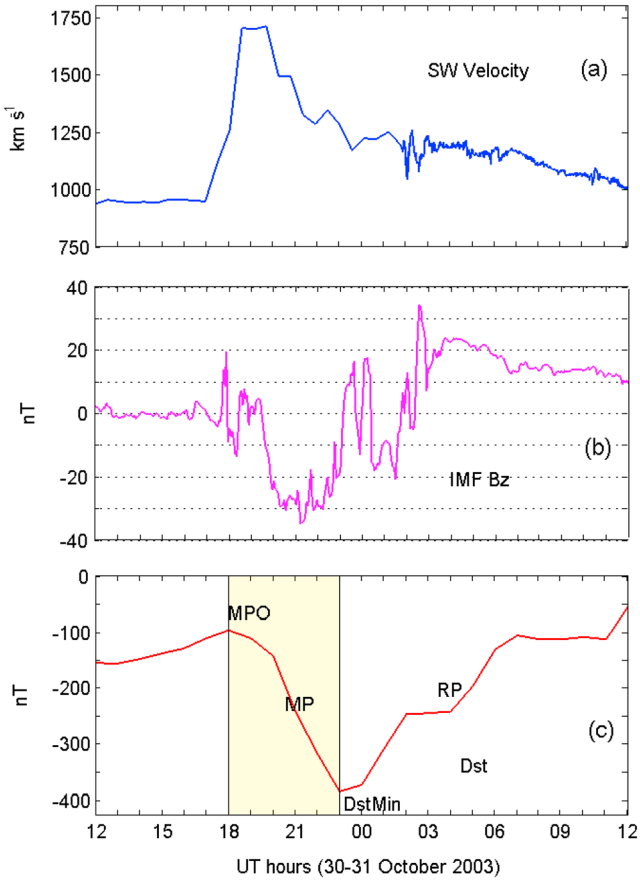

Figure 1. (a) Solar wind velocity *V*, (b) IMF B_z, and (c) *Dst* during the space weather event on 30–31 October 2003. Colored part in Figure 1c indicates storm main phase (MP).

2. Definition

As mentioned in section 1, *severe space weather* (SvSW) events are defined as those events that caused electric power outages and/or telegraph system failures. Five such SvSW events have been known: the Carrington event of September 1859, the Quebec event of March 1989, the New Zealand event of November 2001, the Halloween event of October 2003, and an event in February 1958, which will be denoted by the letters C, Q, N, H, and F, respectively. All other space weather events that did not cause such severe effects are considered *normal space weather* (NSW) events.

The CME front (or CME shock) is defined as the time when the solar wind velocity suddenly increases to high values (Figure 1). The increase in general is found to take place within ~2 h to reach highest value. The CME front (or shock) velocity (ΔV) is the difference between the mean velocity for 2 h after and 2 h before the start of the velocity increase.

2.1. SvSW Events

The most famous space weather event, the Carrington event, occurred on 1–2 September 1859. On 1 September Carrington spotted a cluster of enormous dark spots (sunspots) on the Sun, and two patches of intensely bright and white light (solar flares) erupted from the sunspots. The flares lasted for only 5 min and their effects were felt across the globe within hours. For example, telegraph communications failed and brilliant auroras occurred [*Carrington*, 1859]; electricity was not widely used at that time. More importantly, the most extreme geomagnetic storm in known history occurred. The main phase (MP) of the storm [*Tsurutani et al*., 2003] has a short duration of only about 2 h with no fluctuations; it has the highest values of *H* range ~1710 nT, mean *H* range ~700 nT, and $(dH/dt)_{MP}$ ~1390 nT/h. These extreme characteristics indicate that a huge amount of energy was put into geospace in a short duration so that the geospace responded impulsively. However, *Akasofu and Kamide* [2005] pointed out several reasons to believe that the high value of *Dst*Min (−1760 nT) calculated by *Tsurutani et al*. [2003] for this storm is unrealistic though it remains as the most extreme in known history. *Cliver and Svalgaard* [2004] estimated the solar wind velocity for the Carrington event and other major space weather events since 1859 by considering the magnetic crochet amplitude, solar energetic proton fluence, Sun-Earth disturbance transit time, geomagnetic storm intensity, and low-latitude auroral extent. The estimates provide a high solar wind velocity *V* of ~2250 km s^{-1} for the Carrington event, which gives a ΔV of ~1850 km s^{-1}. An average southward IMF B_z of −50 nT is assumed.

The famous electric power outage in Quebec happened on 13 March 1989. The SvSW event struck at ~07:44 UT, and the Hydro-Quebec electric power grid collapsed in less than 2 min resulting in the loss of electric power to more than six million people for 9 h at an economic cost estimated to be around 13.2 billion Canadian dollars [*Medford et al*., 1989; *Boteler et al*., 1998; *Bolduc*, 2002]. The power outage coincided with the peak of impulsive powerful solar proton flux [*Shirochkov et al*., 2015] and sudden storm commencement of an

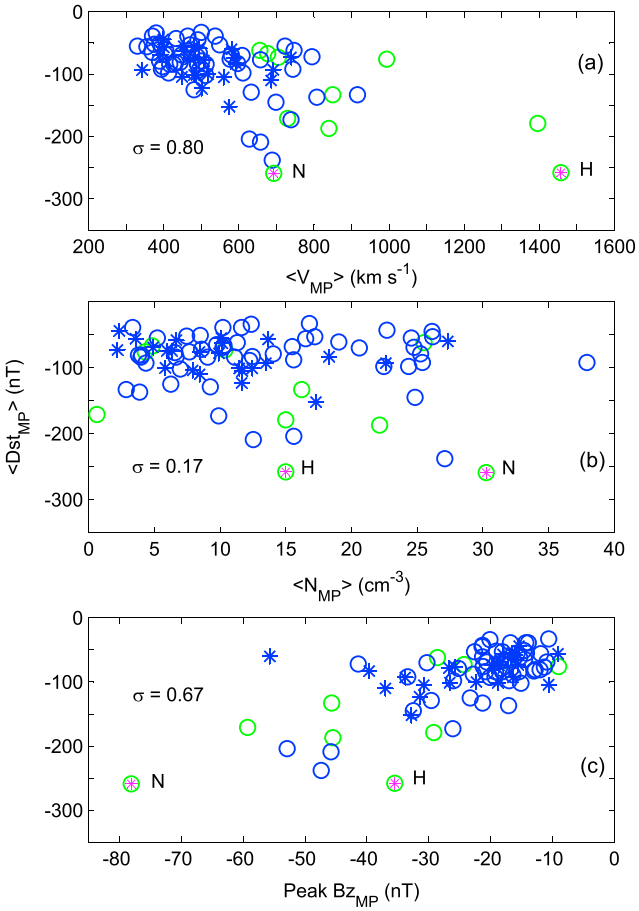

Figure 2. Scatterplots of (a) $<V_{MP}>$, (b) $<N_{MP}>$, and (c) peak B_{zMP} during the MP of 89 intense *Dst* storms in 1998–2016 against $<Dst_{MP}>$. Blue and green symbols indicate data corresponding to SWI and SSTI modes of the ACE/SWEPAM instrument, stars and circles represent IMF B_z southward and northward (or fluctuating) at the CME front (or shock), and green circles with purple stars inside are SvSW events.

extreme geomagnetic storm [*Fujii et al.*, 1992]. The extreme *Dst* storm has $<Dst_{MP}>$ of −310 nT and *Dst*Min −589 nT with MPO at 10 UT. *Nagatsuma et al.* [2015] estimated the solar wind velocity and IMF B_z during the event using the magnetic field variations at the magnetosheath measured by geosynchronous satellites and dawn to dusk solar wind electric field (VB_z) estimated from *Dst* index using an empirical formula for *Dst* prediction [*O'Brien and McPherron*, 2000]. The estimates give solar wind velocity of 960 km s^{-1} and IMF B_z of −50 nT; ΔV of 560 km s^{-1} and average IMF B_z at ΔV of −30 nT are assumed.

The SvSW events on 6 November 2001 and 30 October 2003 caused power outages in New Zealand at ~01:53 UT [*Marshall et al.*, 2012] and Sweden at ~20:07 UT [e.g., *Pulkkinen et al.*, 2005]. The power outages occurred immediately after the impact of the CME fronts (or CME shocks). The events also produced extreme *Dst* storms of $<Dst_{MP}>$ <−250 nT. All data are available for both these events. The SvSW event on 11 February 1958 caused fire and severe damages in the telegraph systems in Sweden [e.g., *Wik et al.*, 2009]. *Cliver et al.* [1990] estimated the maximum solar wind velocity at the Earth during this and other major space weather events since 1938 by calculating the average speed of the associated interplanetary shocks from the time intervals between the flares and onsets of the geomagnetic storms. The estimates give a solar wind velocity of ~1100 km s^{-1} for the 11 February 1958 event; ΔV of 700 km s^{-1}, and average IMF B_z of −25 nT at ΔV and −35 nT at MP are assumed. The associated extreme *Dst* storm has $<Dst_{MP}>$ of −275 nT and *Dst*Min of −426 nT. As described, all SvSW events are associated with high ΔV (>275 km s^{-1}) and large IMF B_z southward. They all produced extreme *Dst* storms of large $<Dst_{MP}>$ (<−250 nT).

3. Data and Analysis

Continuous solar wind and IMF data since 1998 are provided by the ACE satellite at the L1 point between the Sun and Earth. The solar wind velocity and density data available at Caltech (http://www.srl.caltech.edu/ACE/ASC/) are measured by the SWI (Solar Wind Ion) mode of the SWEPAM (Solar Wind Electron, Proton, and Alpha Monitor) instrument at 64 s resolution [e.g., *McComas et al.*, 1998; *Skoug et al.*, 2004]. During high-energy particle events, since SWI mode may not cover the full solar wind flux distribution, the 64 s data are also collected in another mode called SSTI (Search/Supra Thermal Ion) mode once every ~32 min. We use the SSTI data when SWI data are not available. The ACE data are time shifted to the Earth based on the ACE-Earth distance and solar wind velocity. Since measured solar wind and

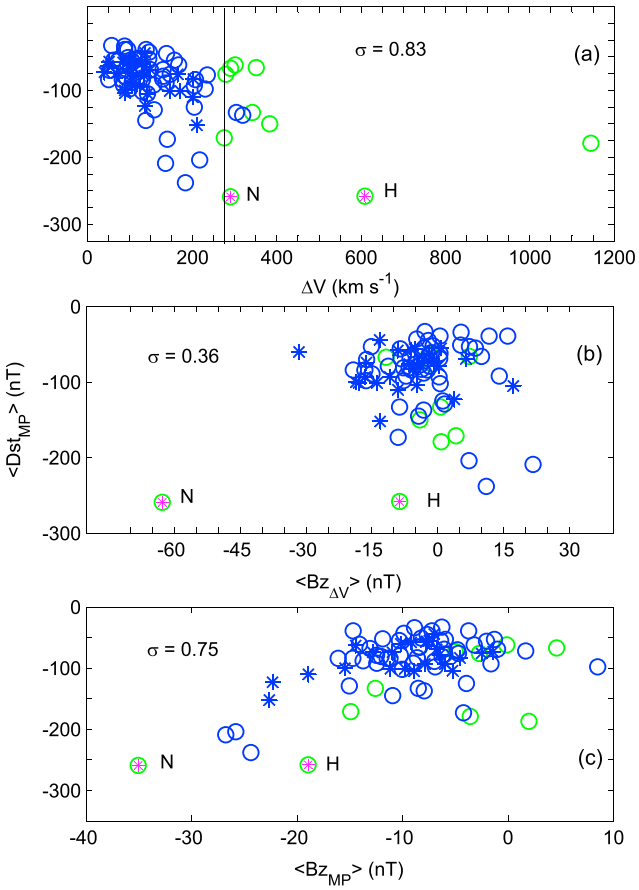

Figure 3. Scatterplots of (a) ΔV, (b) $<B_{z\Delta V}>$, and (c) $<B_{zMP}>$ during the MP of 89 intense *Dst* storms against $<Dst_{MP}>$.

IMF data are not available for the Carrington, Quebec, and February 1958 SvSW events, we use the information (section 2) available in the literature [e.g., *Cliver et al.*, 1990; *Cliver and Svalgaard*, 2004; *Nagatsuma et al.*, 2015].

The severity of space weather depends on the energy input into the magnetosphere, which takes place mainly through magnetic reconnection between southward (or negative) IMF B_z and the northward magnetopause magnetic field [e.g., *Borovsky et al.*, 2008], which also produces the main phase (MP) of *Dst* storms. *Dst* data available at Kyoto WDC (World Data Center) http://wdc.kugi.kyoto-u.ac.jp/dstdir/ are therefore used to identify space weather events. All major space weather events in 1998–2016 that produced 89 intense *Dst* storms (*Dst*Min ≤ -100 nT) are identified.

Solar wind and IMF data are analyzed to obtain all parameters needed for developing the forecast scheme. The MP duration T_{MP} (Figure 1) from MPO (main phase onset) when *Dst* starts decreasing until it reaches *Dst*Min is obtained for all storms. The mean values of solar wind velocity V, density N, and dynamic pressure P and IMF B_z corresponding to T_{MP} are calculated as $<V_{MP}> = (1/T_{MP})\int_{TMP} V dt$, $<N_{MP}> = (1/T_{MP}) \int_{TMP} N dt$, $<P_{MP}> = (1/T_{MP}) \int_{TMP} P dt$, and $<B_{zMP}> = (1/T_{MP}) \int_{TMP} B_z dt$. The CME front (or shock) velocity (ΔV, section 2) is the difference between the mean velocity for 2 h after and 2 h before the start of velocity increase. The corresponding mean B_z at ΔV ($<B_{z\Delta V}>$) is calculated. Peak values of all parameters during MP are also obtained.

4. Forecast Scheme

The 89 major space weather events since 1998 are grouped into two categories: IMF B_z southward at CME front (26 events, for example, Figure 1) and IMF B_z fluctuating or northward at CME front (63 events), which will be shown by stars and circles, respectively. The SvSW events since 1998 will be shown by purple stars inside circles and those earlier by different symbols. The SSTI and SWI data from ACE are identified by green and blue color symbols, respectively.

Figure 2 shows scatterplots of $<V_{MP}>$, $<N_{MP}>$, and peak B_{zMP} of all 89 events against $<Dst_{MP}>$ as a reference. The two SvSW events (H and N) have larger $<Dst_{MP}>$ than the 87 NSW events. Figure 3 is similar to Figure 2 but for ΔV, $<B_{z\Delta V}>$,and $<B_{zMP}>$. Both SvSW events have $\Delta V > 275$ km s^{-1} (Figure 3a); and ACE SWI mode switched to SSTI mode when ΔV exceeded ~275 km s^{-1} in all 12 cases except in two (26 July 2004 and 14 December 2006) though ΔV was 304 km s^{-1} and 320 km s^{-1}, because the energetic charged particle density was low and so SWI mode data remained valid.

The main observation in Figures 2 and 3 is that none of the parameters shown on the X axes individually can identify SvSW as there are a large number of NSW events between the two SvSW events. At the same time we

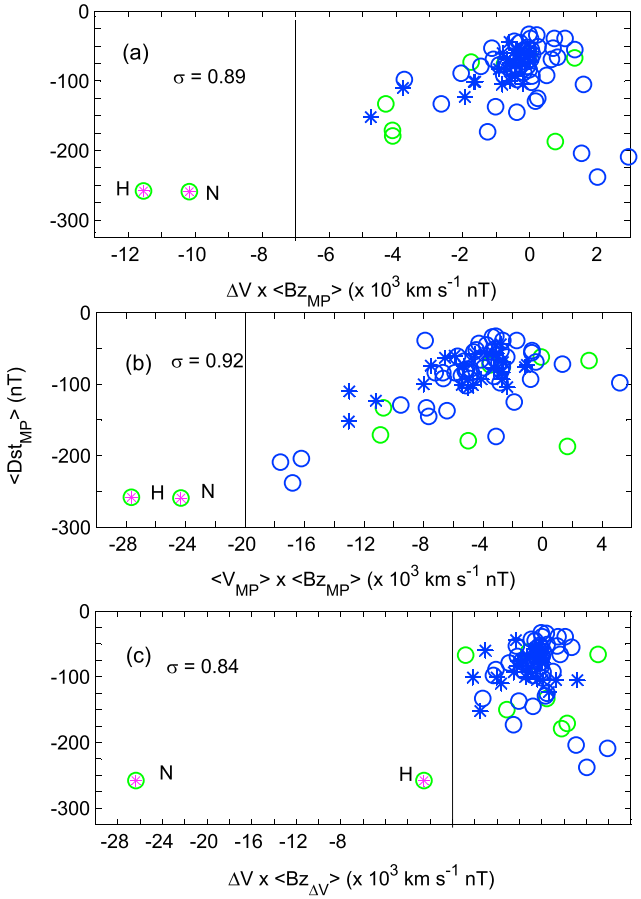

Figure 4. Scatterplots of (a) ($\Delta V \times \langle B_{zMP} \rangle$), (b) ($\langle V_{MP} \rangle \times \langle B_{zMP} \rangle$), and (c) ($\Delta V \times \langle B_{z\Delta V} \rangle$) of 89 major space weather events against $\langle Dst_{MP} \rangle$.

know that the main parameters involved in magnetic reconnection at the magnetopause and hence space weather in the Earth's environment are ΔV, $\langle B_{z\Delta V} \rangle$, $\langle V_{MP} \rangle$,and $\langle B_{zMP} \rangle$. These parameters are selected for developing the forecast scheme. Between peak B_{zMP} (Figure 2c) and $\langle B_{zMP} \rangle$ (Figure 3c), $\langle B_{zMP} \rangle$ is selected because it has fewer NSW events between the two SvSW events and higher correlation (0.75) than peak B_{zMP} (0.67) with $\langle Dst_{MP} \rangle$.

Figure 4 reveals the main result. Combinations of important parameters can clearly distinguish SvSW and NSW events. The product ($\Delta V \times \langle B_{zMP} \rangle$, Figure 4a) has a large margin between SvSW and NSW events of over 5 units on a scale of 12 units, ($\langle V_{MP} \rangle \times \langle B_{zMP} \rangle$, Figure 4b) has a margin of ~6 units on a scale of 28 units, and ($\Delta V \times \langle B_{z\Delta V} \rangle$, Figure 4c) has a margin of ~2 units on a scale of 26 units. The combination ($\Delta V \times \langle B_{zMP} \rangle$) seems best for forecasting as it shows better margin on a shorter scale. It is interesting to note that the products ($\langle V_{MP} \rangle \times \langle B_{zMP} \rangle$, Figure 4b) of the two SvSW events containing high ΔV ($>275\,km\,s^{-1}$) in $\langle V_{MP} \rangle$ only are separated from the corresponding products of all 87 NSW events, even though a number of the NSW events also have high $\langle V_{MP} \rangle$ ($>695\,km\,s^{-1}$). This is mainly because the NSW events which have high $\langle V_{MP} \rangle$ are generally associated with small $\langle B_{zMP} \rangle$ (compare green circles in Figures 2a and 3c) due to long MP. A few NSW events which have large $\langle B_{zMP} \rangle$ are associated with small $\langle V_{MP} \rangle$. Also, only 26 out of 89 events have B_z southward at ΔV, and only 2 out of 12 events with high ΔV ($>275\,km\,s^{-1}$, Figure 3a) have sufficiently large B_z southward at ΔV. In other words, only 2 out of 89 major space weather events including 14 super events ($Dst\text{Min} \leq -250$ nT) since 1998 caused SvSW, discussed in section 5. The correlation coefficients of the products of the important parameters with $\langle Dst_{MP} \rangle$ (Figure 4) are also higher than those of the individual parameters (Figures 2 and 3).

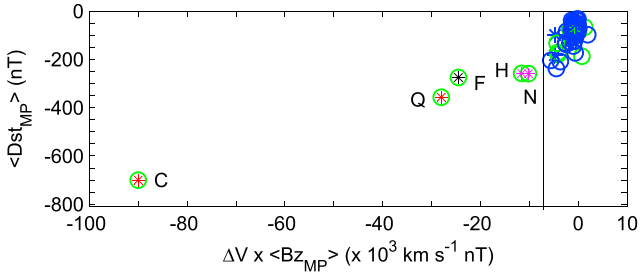

Figure 5. Scatter plot of ($\Delta V \times \langle B_{zMP} \rangle$) against $\langle Dst_{MP} \rangle$ including the Carrington event, the Quebec event, and the February 1958 event.

Figure 5 is similar to Figure 4a but includes Carrington and Quebec events (red stars) and February 1958 event (black star). The ΔV values of these events are obtained from models [e.g., *Cliver et al.*, 1990; *Cliver and Svalgaard*, 2004; *Nagatsuma et al.*, 2015], the B_z value of the Quebec event is also from a model [*Nagatsuma et al.*, 2015], and for other two events B_z values are assumed (section 2). The

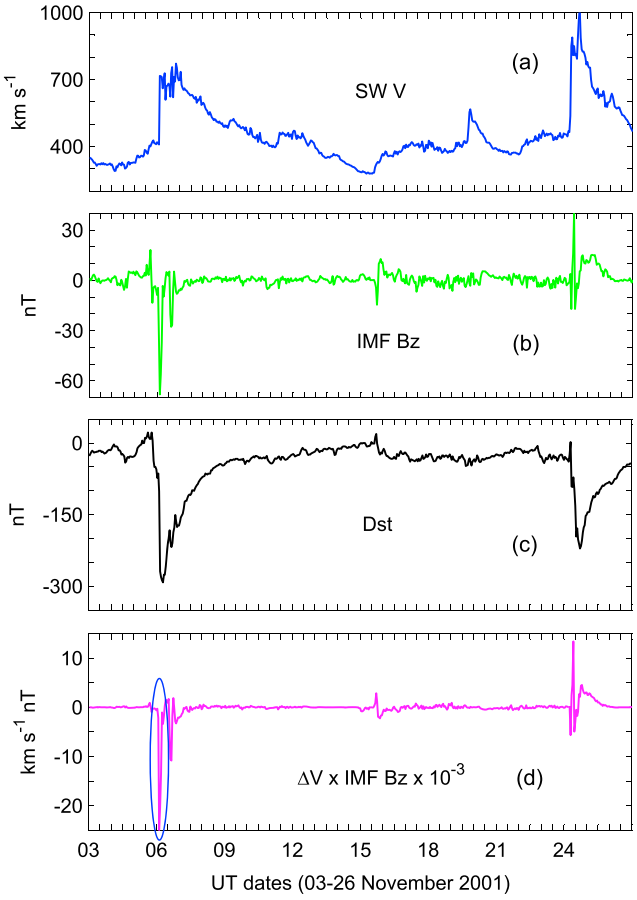

Figure 6. Variations of hourly values of (a) V, (b) B_z, (c) Dst, and (d) $(\Delta V \times B_z)$ during 3–26 November 2001 with $\Delta V = (V - 400)$ and $(V - 450)$ for the periods before and after 15 November. The large negative spike in Figure 6d on 6 November corresponds to SvSW in New Zealand.

result in Figure 5 is similar to that in Figure 4; that is, the product $(\Delta V \times <B_{zMP}>)$ can clearly distinguish between SvSW and NSW events and hence can be used for forecasting SvSW. The product $(\Delta V \times <B_{zMP}>)$ involves the durations of ΔV (2 h) and $<B_{zMP}>$ (short to long hours). This difficulty will be overcome when the forecast scheme is tested and used.

Next the forecast scheme is tested. Figure 6 displays the product $(\Delta V \times B_z)$ using hourly values V and B_z in November 2001 when two CMEs flew past the Earth with high front velocity ΔV of 290 km s^{-1} on 6 November and 383 km s^{-1} on 24 November; $\Delta V = (V - 400)$ and $(V - 450)$ are used for the periods before and after 15 November; these ΔV values correspond to those of the CMEs on 6 November and 24 November, respectively. The product $(\Delta V \times B_z)$ shows a large and distinct negative spike at ΔV on 6 November (Figure 6c) when an electric power outage happened in New Zealand [*Marshall et al.*, 2012]. The product on 24 November is positive at ΔV due to positive B_z and no SvSW occurred.

Figure 7 is similar to Figure 6 but for the Halloween period from 26 October to 25 November 2003 when three CMEs flew past the Earth with high front velocity ΔV of ~1145 km s^{-1} on 29 October, 610 km s^{-1} on 30 October and 220 km s^{-1} on 20 November; $\Delta V = (V - 850)$ and $(V - 410)$ are used for the periods before and after 10 November. The product $(\Delta V \times B_z)$ shows a large and distinct negative spike on 30 October (Figure 7c) when an electric power outage happened in Sweden [*Pulkkinen et al.*, 2005]. On 29 October and 20 November when SvSW did not occur, the product is positive at ΔV due to positive B_z. The product, however, does become negative, but away from ΔV, and the negative excursions are comparatively broad and weak due to the extended intervals of long $-B_z$, which resulted in long superstorms (DstMin = −353 nT and −422 nT).

The large negative spikes on 6 November 2001 and 30 October 2003 when power outages occurred exceeded a threshold of −15 units (Figures 6 and 7), and these spikes have large separation from other minor negative spikes. The product $(\Delta V \times B_z)$ exceeding a threshold (−15 units) therefore seems to be a good index for forecasting SvSW. In addition to using measured ΔV, both SvSW events are tested using a common ΔV of $(V - 400)$ corresponding to average V of 400 km s^{-1}. The results are found to be similar though the sharp negative spike at ΔV on 30 October 2003 falls below −25 units instead of below −20 units.

5. Discussion

As introduced in section 1, the product VB_z has been used previously for forecasting Dst storms. For example, the algorithm developed by *Burton et al.* [1975] using V, N, and B_z successfully forecasted the signature of

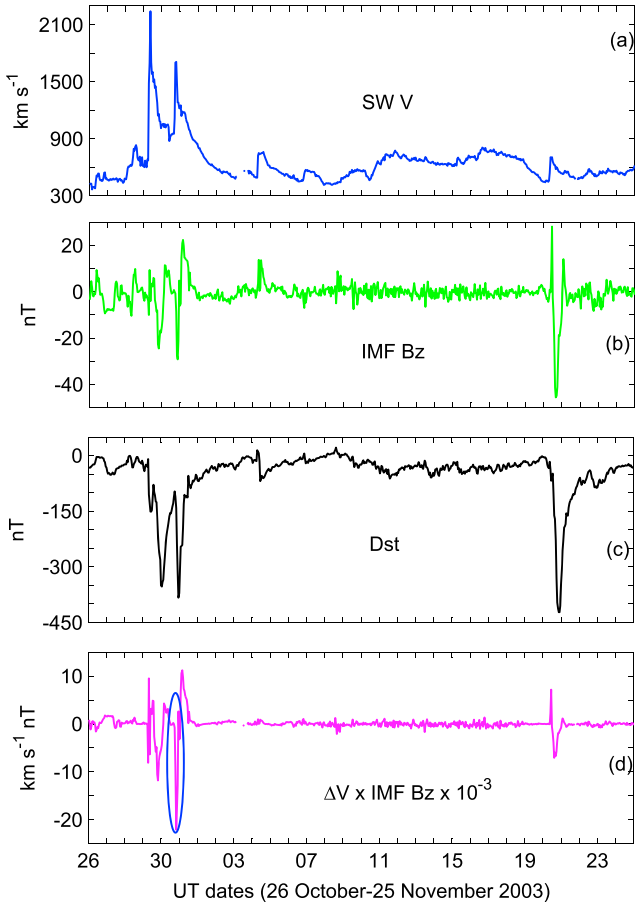

Figure 7. Variations of hourly values of (a) V, (b) B_z, (c) Dst, and (d) $(\Delta V \times B_z)$ during 26 October to 25 November 2003 with $\Delta V = (V - 850)$ and $(V - 410)$ for the periods before and after 10 November. The large negative spike in Figure 7d on 30 October corresponds to SvSW in Sweden.

seven *Dst* storms in 1967–1968. *Klimas et al.* [1997] showed that the input (V and B_z) and output (*Dst*) of their local-linear and nonlinear dynamical analogues of the forecast model couple to the solar wind through the expression $(VB_z/Dst) \times VB_z$ rather than through linear dependence on VB_z. *Zhu et al.* [2007] found that their multi-input (VB_z and P) and single-output (*Dst*) discrete time model can forecast *Dst* dynamics more accurately than previous models. We calculated the CME-magnetosphere coupling function of *Newell et al.* [2007] for all 89 major space weather events since 1998 as before [*Balan et al.*, 2014]. However, it is found not able to distinguish between SvSW and NSW events (not shown) though it is a good measure of the efficiency of CME-magnetosphere coupling. As mentioned in section 1, earlier studies were not designed for forecasting SvSW.

The present paper (section 4) shows that the product $(\Delta V \times B_z)$ exhibiting a sharp and distinct negative spike exceeding a threshold (-15 units) at ΔV can be used for forecasting SvSW. However, only 2 out of the 89 major space weather events since 1998 were SvSW. This is found to be due to B_z generally being fluctuating or northward at ΔV as illustrated in Figure 8 which displays the V and B_z of six super events ($Dst\text{Min} < -250$ nT). Only in the two SvSW events (Figures 8a and 8b) does sufficiently large $-B_z$ coincide with high ΔV. In other cases B_z is northward or fluctuating at ΔV. Figure 8 also clarifies that high V and large $-B_z$ not containing ΔV may not lead to SvSW (Figures 8c–8f) because the solar wind-magnetosphere coupling then misses the required impulsive action that comes through when V contains high ΔV. Also, if B_z would not have fluctuated at high ΔV (or at CME shock), there would have been 50-50 chance for B_z southward-northward at CME front. In other words a number of SvSW events (more than two since 1998) would have occurred, provided there is 50-50 chance for southward-northward B_z at CME front at its ejection from the Sun. In short, *nature* (background solar wind) seems to protect Earth from the severe effects of space weather. It is also possible that it may be the CME sides (and not their fronts) where B_z is positive that impact the Earth in some cases.

As mentioned in section 1, the severity of space weather depends on the amount and duration of energy input. The process of energy input involves rapid and vigorous magnetic reconnection in the dayside between IMF B_z southward and the northward magnetospheric magnetic field that opens the magnetopause [e.g., *Borovsky et al.*, 2008] through which a fast CME front (or CME shock) impulsively pushes the high-energy plasma inside. This, in turn, through other processes in the magnetosphere-ionosphere system [e.g., *Singh et al.*, 2010] leads to SvSW. Figure 9 illustrates the relationship between energy input and duration. The Y axis ($<P_{MP}> \times <B_{zMP}> \times T_{MP}$) is proportional to energy input, and the X axis shows the duration of energy input. All five SvSW events fall in the bottom left-hand corner. Although the parameters used for the events before 1998 have some uncertainties, the message is clear. That is, the higher

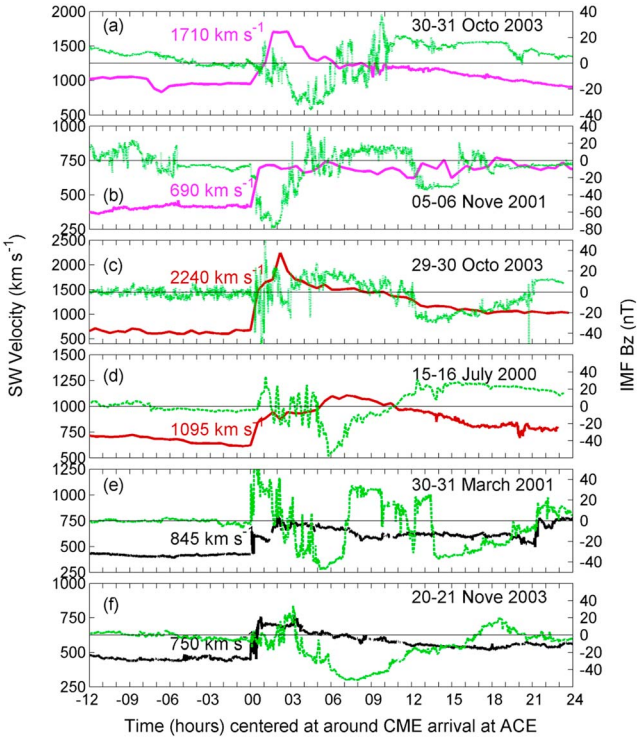

Figure 8. (a and b) Variations of V and B_z (green) for six events illustrating the coincidence of large B_z southward and high ΔV corresponding to SvSW, and (c–f) coincidence of large B_z southward and high V not corresponding to SvSW.

the energy input and the shorter the duration the more severe the space weather, analogous to faster weather fronts and tsunami fronts causing more severe damage through impulsive action. The processes include high rate of change of geomagnetic field, though the maximum change as seen in *Dst* during MP $((dDst/dt)_{MPmax})$ independently is found insufficient to indicate SvSW [*Balan et al.*, 2016]. However, the new parameter $<Dst_{MP}>$ that involves $(dDst/dt)_{MPmax}$, T_{MP}, and *Dst*Min is found unique in indicating SvSW. The Quebec event (Q) seems to have the highest energy and longest duration (Figure 9). If this energy were put into geospace in a shorter duration, it would have caused much more damage than it actually caused in March 1989.

5.1. Model Calculations

The requirement of the coincidence of sufficiently large $-B_z$ at high ΔV for SvSW is tested using the CRCM (Comprehensive Ring Current Model) [*Fok et al.*, 2001]. The model has been used for studying the relative importance of different physical mechanisms that lead to several super *Dst* storms [e.g., *Ebihara et al.*, 2005]. For the present purpose, the model is run for the space weather event on 24 November 2001, which caused NSW (*Dst*Min = −221 nT and $<Dst_{MP}> = -150$ nT). After running the model for the measured values of V and B_z as inputs, the inputs are modified to test if sufficiently large $-B_z$ at high ΔV can lead to SvSW (or produce $<Dst_{MP}> < -250$ nT).

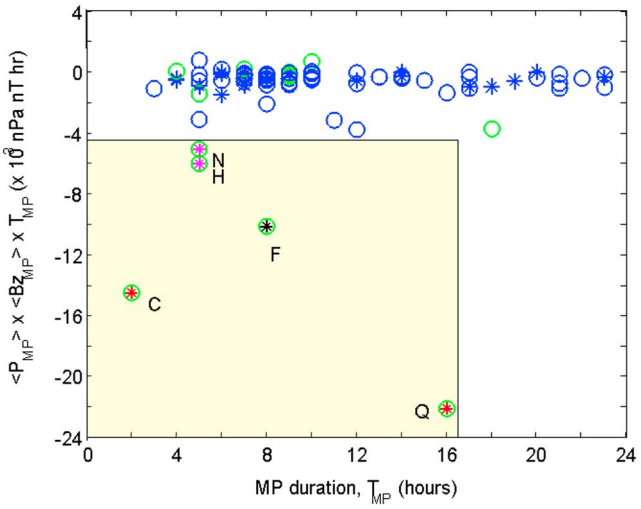

Figure 9. Scatterplot of the product $(<P_{MP}> \times <B_{zMP}> \times T_{MP})$ against T_{MP} of all 92 major space weather events. SvSW events have high-energy input in a short duration.

To model the ring current properly, we need to solve the evolution of the phase space density of the ions that constitute the carrier of the ring current. To do so, we need to take into consideration, at least, the dipolar magnetic field, the convection electric field, the corotation electric field, and the adequate phase space density of plasma sheet ions [*Ebihara and Ejiri*, 2003]. The convection electric field is provided by the empirical model that was developed by *Weimer* [2001]. This empirical model depends on the solar wind speed, density, and IMF. In addition to the dipole magnetic field, we used the T96 magnetic field model [*Tsyganenko*, 1995; *Tsyganenko and Stern*, 1996] that depends on the

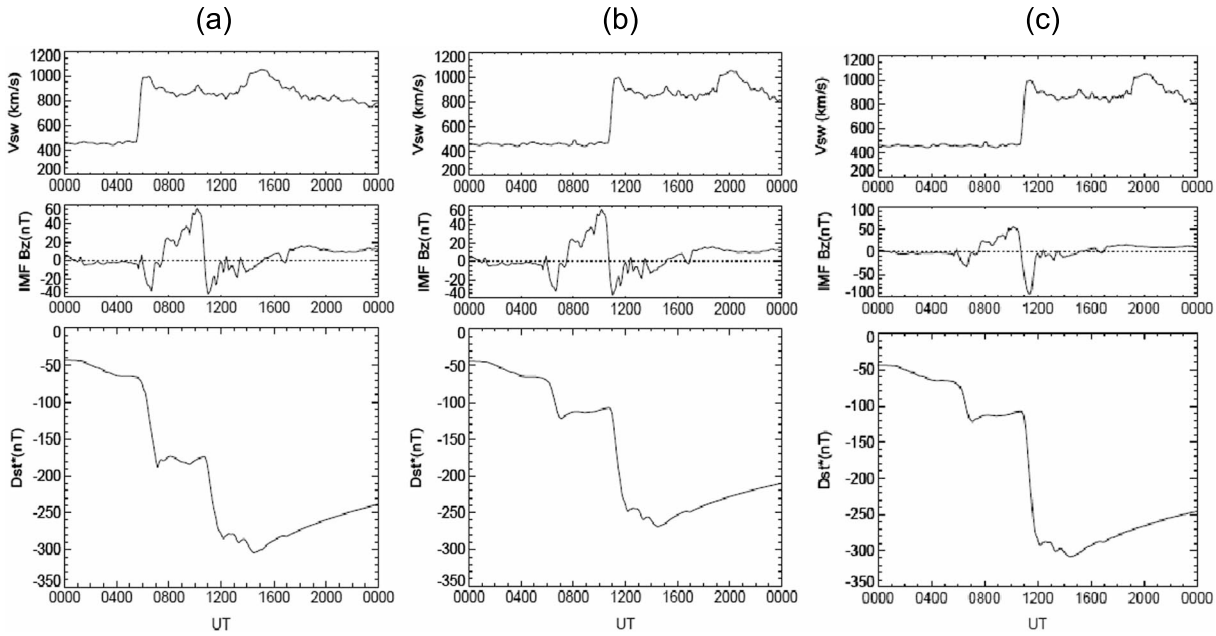

Figure 10. Model *Dst* calculated using CRCM for 24 November 2001 with (a) measured V and B_z as inputs, (b) V shifted to coincide with large B_z southward, and (c) shifted V and large B_z southward nearly doubled.

solar wind dynamic pressure, *Dst*, and IMF. The values observed at 0000 UT on 24 November 2001 were used to drive the T96 magnetic field model. This means that the magnetic field was kept constant over time for this particular simulation. The plasma sheet density and temperature were held constant to be 0.86 cm^{-3} and 6 keV, respectively.

Figure 10 shows the model inputs and outputs for three runs. The measured inputs V and B_z (Figure 10a, top and middle) have a smaller $-B_z$ at high ΔV and a larger $-B_z$ at high V. The *Dst* output (Figure 10a, bottom) qualitatively agrees with *Dst* data. More importantly, the smaller $-B_z$ at high ΔV produces a (slightly) larger sharp *Dst* decrease than that produced by the larger $-B_z$ at high V. The model calculations are repeated by shifting V so that the large ΔV increase coincides with larger $-B_z$ (Figure 10b). The resulting *Dst* has a larger sharp *Dst* decrease at ΔV compared to Figure 10a. The model run of Figure 10b (with shifted V) is repeated by doubling the peak value of $-B_z$ at ΔV. The resulting *Dst* (Figure 10c) now has a much larger sharp decrease at ΔV, with $<Dst_{MP}> < -250$ nT. These results clearly illustrate that it is the coincidence of sufficiently large $-B_z$ at high ΔV that leads to SvSW including extreme *Dst* storms as observed.

The time duration of 2 h used for ΔV in the development of the forecasting scheme may not be a constraint when the velocity V increases rapidly within no time, as is usually the case for SvSW. The product $(\Delta V \times B_z)$ will then suddenly exceed a threshold. The product $(\Delta V \times B_z)$ will exceed the observed threshold of -15 units when the velocity V increases suddenly, for example, by 300 km s^{-1}, 600 km s^{-1}, or 1200 km s^{-1} when B_z is ~-50 nT, -25 nT, or -12.5 nT, respectively. This forecasting scheme can provide a forecast time of less than ~35 min (V = ~675 km s^{-1}) using ACE data (220 R_E away from the Earth). The solar wind and IMF would need to be measured closer to the Sun for better forecast time. Additionally, the advantages of observing CMEs clearly and completely in side views from the L4 and/or L5 points between the Sun and Earth [*Gopalswamy et al.*, 2011] may be considered.

6. Conclusions

A scheme is suggested and tested for forecasting severe space weather (SvSW) that caused all known electric power outages and telegraph system failures using solar wind velocity (V) and north-south component (B_z) of interplanetary magnetic field (IMF) measured using the ACE satellite in 1998–2016. Earlier SvSW events such as the Carrington event of 1859, the Quebec event of 1989, and an event in 1958 are included with

information from the literature. *Dst* storms are used as references to identify 89 major space weather events (*Dst*Min ≤ -100 nT) in 1998–2016. The characteristics of V and B_z that caused all 92 events are calculated, such as CME front (or shock) velocity ΔV (sudden increase in V over the background), mean B_z at ΔV ($<B_{z\Delta V}>$), mean values of V ($<V_{MP}>$), and B_z ($<B_{zMP}>$) during main phase (MP) of *Dst* storms.

The results reveal that (1) large B_z southward coincides with high ΔV (>275 km s^{-1}) in all SvSW events; (2) large B_z southward coinciding with high V (not containing ΔV) does not correspond to SvSW events; (3) products ($\Delta V \times <B_{z\Delta V}>$), ($\Delta V \times <B_{zMP}>$), and ($<V_{MP}> \times <B_{zMP}>$) of all five SvSW events are distinctly separated from those of all 87 normal space weather (NSW) events that did not cause electric power outages and telegraph system failures; (4) separation between SvSW and NSW events is larger for ($\Delta V \times <B_{zMP}>$) on a shorter scale; and (5) the product ($\Delta V \times B_z$) when tested exhibits large negative spikes at ΔV during SvSW events. The product ($\Delta V \times B_z$) exceeding a threshold seems suitable for forecasting SvSW. The CRCM model produces extreme *Dst* storms ($<Dst_{MP}> < -250$ nT) characterizing SvSW when large B_z southward coincides with high ΔV, which seems to verify the importance of the impulsive action of large B_z southward and high ΔV required for SvSW that comes through when they coincide.

This forecasting scheme can provide a forecast time of less than ~35 min using ACE data. The solar wind and IMF would need to be measured closer to the Sun for better forecast time.

Acknowledgments

We acknowledge the use of ACE satellite data and Kyoto WDC *Dst* data available at http://www.srl.caltech.edu/ACE/ASC/ and http://wdc.kugi.kyoto-u.ac.jp/dstdir/. N. Balan thanks ISEE of Nagoya University (JSPS KEKENHI grant JP 15H05815), RISH of Kyoto University, and CNPq of Brazil for visiting professor positions. Work at Los Alamos was performed under the auspices of the U.S. Department of Energy, with support from the NASA-ACE program.

References

Akasofu, S.-I., and Y. Kamide (2005), Comment on "The extreme magnetic storm of 1–2 September 1859" by B. T. Tsurutani, W. D. Gonzalez, G. S. Lakhina, and S. Alex, *J. Geophys. Res.*, *110*, A09226, doi:10.1029/2005JA011005.

Baker, D. N. (2002), How to cope with space weather, *Science*, *297*, 1486–1487, doi:10.1126/science.1074956.

Baker, D. N., X. Li, A. Pulkkinen, C. M. Ngwira, M. L. Mays, A. B. Galvin, and K. D. C. Simunac (2013), A major solar eruptive event in July 2012: Defining extreme space weather scenarios, *Space Weather*, *11*, 1–7, doi:10.1002/swe.20097.

Balan, N., K. Shiokawa, Y. Otsuka, T. Kikuchi, D. Vijaya Lekshmi, S. Kawamura, M. Yamamoto, and G. J. Bailey (2010), A physical mechanism of positive ionospheric storms at low and midlatitudes through observations and modeling, *J. Geophys. Res.*, *115*, A02304, doi:10.1029/2009JA014515.

Balan, N., M. Yamamoto, J. Y. Liu, Y. Otsuak, H. Liu, and H. Luhr (2011), New aspects of thermospheric and ionospheric storms revealed by CHAMP, *J. Geophys. Res.*, *116*, A07305, doi:10.1029/2010JA0160399.

Balan, N., R. Skoug, S. Tulasi Ram, P. K. Rajesh, K. Shiokawa, Y. Otsuka, I. S. Batista, Y. Ebihara, and T. Nakamura (2014), CME front and severe space weather, *J. Geophys. Res. Space Physics*, *119*, 10,041–10,058, doi:10.1002/2014JA020151.

Balan, N., I. S. Batista, S. Tulasiram, and P. K. Rajesh (2016), A new geomagnetic storm parameter for the severity of space weather, *Geosci. Lett.*, *3*, 3, doi:10.1186/s40562-016-0036-5.

Barbieri, L. P., and R. E. Mahmot (2004), October–November 2003' space weather and operations lessons learned, *Space Weather*, *2*, S09002, doi:10.1029/2004SW000064.

Barnard, L., M. Lockwood, M. A. Hapgood, M. J. Owens, C. J. Davis, and F. Steinhilber (2011), Predicting space climate change, *Geophys. Res. Lett.*, *38*, L16103, doi:10.1029/2011GL048489.

Bolduc, L. (2002), GIC observations and studies in the Hydro-Québec power system, *J. Atmos. Sol. Terr. Phys.*, *64*, 1793–1802, doi:10.1016/S1364-6826(02)00128-1.

Borovsky, J. E., M. Hesse, J. Birn, and M. M. Kuzentsova (2008), What determines the reconnection rate at the dayside magnetosphere?, *J. Geophys. Res.*, *113*, A07210, doi:10.1029/2007JA012645.

Boteler, D. H., R. J. Pirjola, and H. Nevanlinna (1998), The effects of geomagnetic disturbances on electrical systems at the Earth's surface, *Adv. Space Res.*, *22*, 1–17, doi:10.1016/S0273-1177(97)01096-X.

Burton, R. K., R. L. McPherron, and C. T. Russell (1975), An empirical relationship between interplanetary conditions and *Dst*, *J. Geophys. Res.*, *80*, 4204, doi:10.1029/JA080i031p04204.

Carrington, R. C. (1859), Description of a singular appearance seen in the Sun on September 1, 1859, *Mon. Not. R. Astron. Soc.*, *20*, 13–15, doi:10.1093/mnras/20.1.13.

Cliver, E. W., and L. Svalgaard (2004), The 1989 solar terrestrial disturbances and current limits of extreme space weather activity, *Sol. Phys.*, *224*, 407, doi:10.1007/s11207-005-4980-z.

Cliver, E. W., J. Feynman, and H. B. Garrett (1990), An estimate of the maximum speed of the solar wind, 1938–1989, *J. Geophys. Res.*, *95*, 17,103–17,112, doi:10.1029/JA095iA10p17103.

Ebihara, Y., and M. Ejiri (2003), Numerical simulation of the ring current: Review, *Space Sci. Rev.*, *105*, 377, doi:10.1023/A:1023905607888.

Ebihara, Y., et al. (2005), Ring current and the magnetosphere-ionosphere coupling during the super storm of 20 November 2003, *J. Geophys. Res.*, *110*, A09S22, doi:10.1029/2004JA010924.

Fok, M.-C., R. A. Wolf, R. W. Spiro, and T. E. Moore (2001), Comprehensive computational model of Earth's ring current, *J. Geophys. Res.*, *106*, 8417, doi:10.1029/2000JA000235.

Fujii, R., H. Fukunishi, S. Kokubun, M. Sugiura, F. Tohyama, H. Hayakawa, K. Tsuruda, and T. Okada (1992), Field-aligned current signatures during the March 13–14, 1989 great magnetic storm, *J. Geophys. Res.*, *97*, 10,703–10,715, doi:10.1029/92JA00171.

Gopalswamy, N., S. Yashiro, G. Michalek, H. Xie, R. P. Lepping, and R. A. Howard (2005), Solar source of the largest geomagnetic storm of cycle 23, *Geophys. Res. Lett.*, *32*, L12S09, doi:10.1029/2004GL021639.

Gopalswamy, N., et al. (2011), Earth-affecting solar causes observatory (EASCO): A potential international living with a star mission from Sun-Earth L5, *J. Atmos. Sol. Terr. Phys.*, doi:10.1016/j.jastp.2011.01.013.

Hapgood, M. A. (2011), Towards a scientific understanding of the risk from extreme space weather, *Adv. Space Res.*, *47*, 2059–2072, doi:10.1016/j.asr.2010.02.007.

Kamide, Y., et al. (1998), Current understanding of magnetic storms: Storm-substorm relationships, *J. Geophys. Res.*, *103*, 17,705–17,728, doi:10.1029/98JA01426.
Kappenman, J. G. (1996), Geomagnetic storms and their impact on power systems, *IEEE Power Eng. Rev.*, *16*, 5–8, doi:10.1109/MPER.1996.491910.
Klimas, A. J., D. Vassiliadis, and D. N. Baker (1997), Data-derived analogues of the magnetospheric dynamics, *J. Geophys. Res.*, *102*, 26,993, doi:10.1029/97JA02414.
Lanzerotti, L. J. (2001), Space weather effects on technologies, in *Space Weather*, edited by P. Song, H. J. Singer, and G. L. Siscoe, pp. 11–22, AGU, Washington, D. C.
Liemohn, M. W., M. Jazowski, J. U. Kozyra, N. Ganushkina, M. F. Thomsen, and J. E. Borovsky (2010), CIR versus CME drivers of the ring current during intense magnetic storms, *Proc. R. Soc. A*, *466*, 3305–3328, doi:10.1098/rspa.2010.0075.
Love, J. J., E. J. Rigler, A. Pulkkinen, and P. Riley (2015), On the lognormality of historical magnetic storm intensity statistics: Implications for extreme-event probabilities, *Geophys. Res. Lett.*, *42*, 6544–6553, doi:10.1002/2015GL064842.
MacQueen, R. M., et al. (1974), The outer solar corona as observed from Skylab: Preliminary results, *Astrophys J.*, *187*, L85–L88, doi:10.1086/181402.
Marshall, R. A., M. Dalzell, C. L. Waters, P. Goldthorpe, and E. A. Smith (2012), Geomagnetically induced currents in the New Zealand power network, *Space Weather*, *10*, S08003, doi:10.1029/2012SW000806.
McComas, D. J., S. J. Bame, P. Barker, W. C. Feldman, J. L. Phillips, and P. Riley (1998), Solar Wind Electron Proton Alpha Monitor (SWEPAM) for the Advanced Composition Explorer, *Space Sci. Rev.*, *86*, 563–612, doi:10.1023/A:1005040232597.
McKenna-Lawlor, S. M. P. (2008), Predicted interplanetary shocks/particles at Mars compared with in-situ observations: An overview, *Planet. Space Sci.*, *56*, 1703–1712, doi:10.1016/j.pss.2008.07.031.
Medford, L. V., L. J. Lanzerotti, J. S. Kraus, and C. G. Maclennan (1989), Transatlantic Earth potential variations during the March 1989 magnetic storms, *Geophys. Res. Lett.*, *16*(10), 1145, doi:10.1029/GL016i010p01145.
Nagatsuma, T., R. Kataoka, and M. Kunitake (2015), Estimating the solar wind conditions during an extreme geomagnetic storm: A case study of the event that occurred on March 13–14, 1989, *Earth Planets Space*, *67*, 78, doi:10.1186/s40623-015-0249-4.
Newell, P. T., T. Sotirelis, K. Liou, C.-I. Meng, and F. J. Rich (2007), A nearly universal solar wind-magnetosphere coupling function inferred from 10 magnetospheric state variables, *J. Geophys. Res.*, *112*, A01206, doi:10.1029/2006JA012015.
O'Brien, T. P., and R. L. McPherron (2000), An empirical phase space analysis of ring current dynamics: Solar wind control of injection and decay, *J. Geophys. Res.*, *105*(A4), 7707–7719, doi:10.1029/1998JA000437.
Pulkkinen, A., S. Lindahl, A. Viljanen, and R. Pirjola (2005), Geomagnetic storm of 29–31 October 2003: Geomagnetically induced currents and their relation to problems in the Swedish high-voltage power transmission system, *Space Weather*, *3*, S08C03, doi:10.1029/2004SW000123.
Pulkkinen, T. (2007), Space weather: Terrestrial perspective, *Living Rev. Sol. Phys.*, *4*, 1, doi:10.12942/lrsp-2007-1.
Russell, C. T., et al. (2013), The very unusual interplanetary coronal mass ejection of 2012 July 23: A blast wave mediated by solar energetic particles, *Astrophys. J.*, *770*, 38, doi:10.1088/0004-637X/770/1/38.
Scurry, L., and C. T. Russell (1991), Proxy studies of energy transfer to the magnetopause, *J. Geophys. Res.*, *96*, 9541, doi:10.1029/91JA00569.
Shibata, K., and T. Magara (2011), Solar flares: Magnetohydrodynamic processes, *Living Rev. Sol. Phys.*, *8*, 6, doi:10.12942/lrr-2011-6.
Shirochkov, A. V., L. N. Makarova, V. D. Nilolaeva, and A. L. Kotokov (2015), The storm of March 1989 revisited: A fresh look at the event, *Adv. Space Res.*, *55*, 211–219, doi:10.1016/j.asr.2014.09.010.
Singh, A. K., D. Siingh, and R. P. Singh (2010), Space weather: Physics, effects and predictability, *Surv. Geophys.*, *31*, 581–638, doi:10.1007/s10712-010-9103-1.
Skoug, R. M., J. T. Gosling, J. T. Steinberg, D. J. McComas, C. W. Smith, N. F. Ness, Q. Hu, and L. F. Burlaga (2004), Extremely high speed solar wind: 29–30 October 2003, *J. Geophys. Res.*, *109*, A09102, doi:10.1029/2004JA010494.
Tsubouchi, K., and Y. Omura (2007), Long-term occurrence probabilities of intense geomagnetic storm events, *Space Weather*, *5*, S12003, doi:10.1029/2007SW000329.
Tsurutani, B. T., W. D. Gonzalez, G. S. Lakhina, and S. Alex (2003), The extreme magnetic storm of 1–2 September 1859, *J. Geophys. Res.*, *108*(A7), 1268, doi:10.1029/2002JA009504.
Tsyganenko, N. A. (1995), Modeling the Earth's magnetospheric magnetic field confined within a realistic magnetopause, *J. Geophys. Res.*, *100*(4), 5599, doi:10.1029/94JA03193.
Tsyganenko, N. A., and D. P. Stern (1996), A new-generation global magnetosphere field model, based on spacecraft magnetometer data, *ISTP News lett.*, *6*(1), 21.
Viljanen, A., A. Pulkkinen, R. Pirjola, K. Pajunpaa, P. Posio, and A. Koistinen (2006), Recordings of geomagnetically induced currents and a nowcasting service of the Finnish natural gas pipe line system, *Space Weather*, *4*, S10004, doi:10.1029/2006SW000234.
Weimer, D. R. (2001), An improved model of ionospheric electric potentials including substorm perturbations and application to the Geospace Environment Modeling November 24, 1996, event, *J. Geophys. Res.*, *106*, 407, doi:10.1029/2000JA000604.
Wik, M., R. Pirjola, H. Lundstedt, A. Viljanen, P. Wintoft, and A. Pulkkinen (2009), Space weather events in July 1982 and October 2003 and the effects of geomagnetically induced currents on Swedish technical systems, *Ann. Geophys.*, *27*, 1775–1787, doi:10.5194/angeo-27-1775-2009.
Wu, C.-C., and R. P. Lepping (2002), Effect of solar wind velocity on magnetic cloud-associated magnetic storm intensity, *J. Geophys. Res.*, *107*(A11), 1346, doi:10.1029/2002JA009396.
Zhu, D., S. A. Billings, M. A. Balikhin, S. Wing, and H. Alleyne (2007), Multi-input data derived *Dst* model, *J. Geophys. Res.*, *112*, A06205, doi:10.1029/2006JA012079.